Extreme Mechanics Letters 3 (2015) 66–71

Contents lists available at ScienceDirect

Extreme Mechanics Letters

journal homepage: www.elsevier.com/locate/eml

180° magnetization switching in nanocylinders by a mechanical strain

Min Yi [a,*], Bai-Xiang Xu [b,*], Zhigang Shen [a]

[a] School of Aeronautic Science and Engineering, Beijing University of Aeronautics and Astronautics, Xueyuan Road 37, Beijing 100191, China

[b] Mechanics of Functional Materials Division, Institute of Materials Science, Technische Universität Darmstadt, Jovanka-Bontschits-Strasse 2, Darmstadt 64287, Germany

ARTICLE INFO

Article history:
Received 11 February 2015
Received in revised form 9 March 2015
Accepted 10 March 2015
Available online 12 March 2015

Keywords:
Magneto-mechanical coupling
180° switching
Nanomagnets

ABSTRACT

The magnetization switching dynamics in ferromagnetic Cobalt nanocylinders under mechanical loading is studied by a constraint-free phase field model, which allows the exactly constant magnetization magnitude and the explicit magneto-mechanical coupling. Results show that the single-domain switching mode, which is of great interest for memory technologies, exists only in small nanocylinders, and the critical radius is found to be around 8 nm. Furthermore, a novel mechanical loading and unloading scheme, which makes use of the overrun of magnetization during the precessional switching, is proposed to achieve a deterministic 180° switching. The 180° switching is driven firstly by the magneto-mechanical coupling and then by the magnetocrystalline anisotropy (K_u). The threshold strain to induce the deterministic switching increases with K_u. The switching time firstly decreases with increasing strain rapidly and then saturates. The results shed light on the design of an optimum mechanically driven nanomagnets-based logic and memory devices.

1. Introduction

Along with the miniaturization of magnetic memory cells, the nanomagnet-based bit patterned media (BPM) have been a potential candidate for the next generation of high density memory technologies [1,2]. In the BPM concept, each nanomagnet saves one single bit of information. This requires a 180° switching of the magnetization [3–7], so that the nanomagnet changes its bit state from 0 to 1, or vice versa.

Presently, the 180° switching of magnetization by a magnetic field or the spin-polarized current has been the main-stay. However, the approach by magnetic field has the issue of a large power consumption and the magnetic stray fields that may affect neighboring nanomagnetic cells [8]. The spin-polarized current induced magnetization switching enables much smaller memory cells [9–11]. But the required current density for switching is still large ($1\ \mathrm{MA/cm^2}$) and can cause metal migration [6,8,9].

Electric field control of the switching in multiferroic nanomagnets has recently received significant interests, due to the low power consumption [12–14]. A typical model for realizing this control is a nanomagnetic layer mechanically coupled to an underlying piezo/ferroelectric layer [5,6,14–22]. Thereby the magnetization in the nanomagnetic layer is switched by the mechanical loading transferred from the electroactive piezo/ferroelectric layer. Unfortunately, in most of the proposed multiferroic structures, for the steady-state consideration, mechanical strain can only switch magnetization by 90°. If loading is removed after the magnetization steadily reaches 90°, the

* Corresponding authors.
E-mail addresses: yimin@buaa.edu.cn (M. Yi), xu@mfm.tu-darmstadt.de (B.-X. Xu), shenzhg@buaa.edu.cn (Z. Shen).

http://dx.doi.org/10.1016/j.eml.2015.03.004
2352-4316/

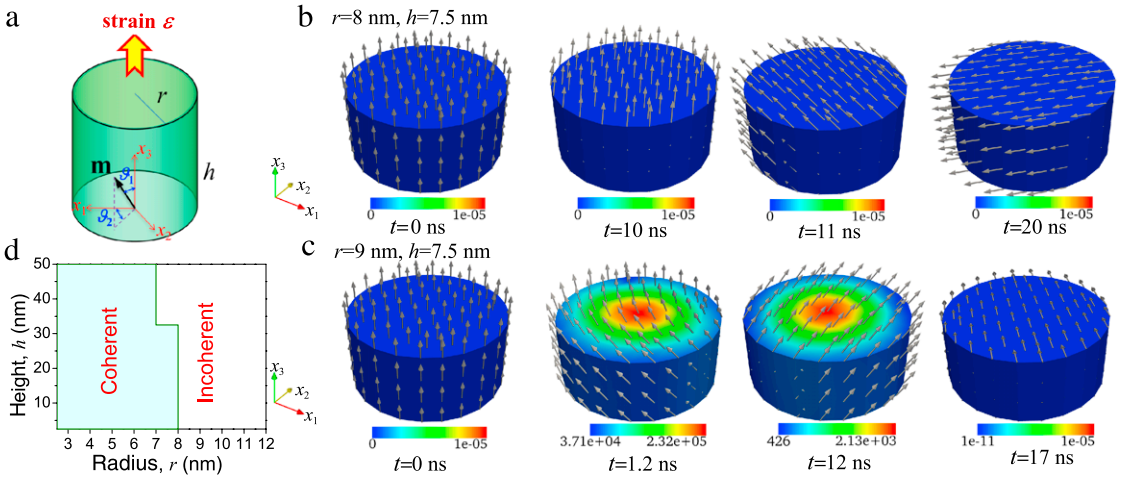

Fig. 1. (a) The hcp Cobalt nanocylindrical model, with x_3 as the easy axis of magnetization. (b) Coherent switching for $r = 8$ nm and $h = 7.5$ nm. (c) Incoherent switching for $r = 9$ nm and $h = 7.5$ nm. The scale bar in (b) and (c) denotes the exchange energy $\mathcal{H}^{\text{exc}}$. (d) Switching mode transition map.

magnetization has equal possibility to revert back to 0° state and to switch by 180°. This has been demonstrated both in theory and experiments [3,5–7,17,22].

In this letter, we demonstrate by constraint-free phase field simulations that a mechanical strain induced deterministic 180° can be achieved by making use of the magnetization overrun beyond 90° during the precessional switching. As a modal example, hexagonal close-packed (hcp) Cobalt nanocylinders are considered. First of all, the size limit, within which the single-domain switching mode (coherent switching) happens, is determined. The novel mechanical loading mechanism is then explained, and the induced magnetization switching is simulated. The dependence of the switching time on the mechanical strain and the magnetocrystalline anisotropy is further explored.

2. Model and simulation

For the study, the constraint-free phase field model is used, which allows explicit magneto-mechanical coupling, mechanical boundary conditions, and a straightforward realization of the constraint on a constant magnetization magnitude. It is known that when the temperature is far below the Curie point, the magnitude of the magnetization vector $\mathbf{M}$ should be constant, i.e. $\mathbf{M} = M_s\mathbf{m}$ with M_s being the constant saturation magnetization and $\mathbf{m}$ the magnetization unit vector. In contrast to the conventional micromagnetic or phase field models, the constraint-free phase field model takes the polar and azimuthal angles $(\vartheta_1, \vartheta_2)$, instead of the Cartesian components (m_1, m_2, m_3) of vector $\mathbf{m}$, as the order parameters, as shown in Fig. 1(a). In this way, the constraint on the magnitude of the magnetization vector is fulfilled automatically, and thus no additional numerical treatment on the constraint is required [23].

In the model, the total magnetic enthalpy for a hcp crystal consists of the magnetocrystalline anisotropy contribution $\mathcal{H}^{\text{ani}}$, the exchange contribution $\mathcal{H}^{\text{exc}}$, the magnetostatic contribution $\mathcal{H}^{\text{mag}}$, the pure mechanical contribution $\mathcal{H}^{\text{mech}}$, and the magneto-elastic coupling contribution $\mathcal{H}^{\text{mag-ela}}$, i.e.

$$\mathcal{H} = \mathcal{H}^{\text{ani}} + \mathcal{H}^{\text{exc}} + \mathcal{H}^{\text{mag}} + \mathcal{H}^{\text{mech}} + \mathcal{H}^{\text{mag-ela}} \tag{1}$$

in which

$$\begin{aligned}
\mathcal{H}^{\text{ani}} &= K_u \sin^2\vartheta_1 \\
\mathcal{H}^{\text{exc}} &= A_e(\vartheta_{1,j}\vartheta_{1,j} + \sin^2\vartheta_1\vartheta_{2,j}\vartheta_{2,j}) \\
\mathcal{H}^{\text{mag}} &= -\frac{1}{2}\mu_0 H_j H_j - \mu_0 M_s(H_1\sin\vartheta_1\cos\vartheta_2 \\
&\quad + H_2\sin\vartheta_1\sin\vartheta_2 + H_3\cos\vartheta_1) \\
\mathcal{H}^{\text{mech}} &= \frac{1}{2}C_{11}(\varepsilon_{11}^2 + \varepsilon_{22}^2) + \frac{1}{2}C_{33}\varepsilon_{33}^2 \\
&\quad + C_{13}(\varepsilon_{11}\varepsilon_{33} + \varepsilon_{22}\varepsilon_{33}) + C_{12}\varepsilon_{11}\varepsilon_{22} \\
&\quad + 2C_{44}(\varepsilon_{23}^2 + \varepsilon_{31}^2) + (C_{11} - C_{12})\varepsilon_{12}^2 \\
\mathcal{H}^{\text{mag-ela}} &= B_1(\sin^2\vartheta_1\cos^2\vartheta_2\varepsilon_{11} + 2\sin^2\vartheta_1 \\
&\quad \times \sin 2\vartheta_2\varepsilon_{12} + \sin^2\vartheta_1\sin^2\vartheta_2\varepsilon_{22}) \\
&\quad + B_2\sin^2\vartheta_1\varepsilon_{33} + B_3\sin^2\vartheta_1 \\
&\quad \times (\varepsilon_{11} + \varepsilon_{22}) + B_4(\sin 2\vartheta_1\sin\vartheta_2\varepsilon_{23} \\
&\quad + \sin 2\vartheta_1\cos\vartheta_2\varepsilon_{31}).
\end{aligned} \tag{2}$$

Here, C_{11}, C_{12}, C_{33}, C_{13}, and C_{44} are the elastic constants. $\varepsilon_{ij} = \frac{1}{2}(u_{i,j} + u_{j,i})$ are the strain with u_i as the mechanical displacement. The Latin indices i and j run over 1–3. Meanwhile, B_1, B_2, B_3, and B_4 are the magneto-elastic coupling coefficients, K_u is the anisotropy constant, A_e is the exchange stiffness constant, and μ_0 is the vacuum permeability. The magnetic field $H_j = -\phi_{,j}$ with ϕ as the magnetic scalar potential.

With the above specified magnetic enthalpy, a combination of the configurational force balance and the second law of thermodynamics leads to a generalized evolution equation for the order parameters ϑ_1 and ϑ_2, which is [23]

$$\frac{1}{M_s}\left(\frac{\partial\mathcal{H}}{\partial\vartheta_{\mu,j}}\right)_{,j} - \frac{1}{M_s}\frac{\partial\mathcal{H}}{\partial\vartheta_\mu} + \zeta_\mu^{\text{ex}} = \frac{1}{\gamma_0}L_{\mu\gamma}\frac{\partial\vartheta_\gamma}{\partial t} \tag{3}$$

with the mobility matrix **L** as

$$L_{\mu\gamma} = \begin{bmatrix} \alpha & -\sin\vartheta_1 \\ \sin\vartheta_1 & \alpha\sin^2\vartheta_1 \end{bmatrix}. \quad (4)$$

In the equation, ζ_μ^{ex} is the external field, α the damping coefficient, and $\gamma_0 = 1.76 \times 10^{11}/(\text{T s})$ the gyromagnetic ratio. The Greek indices μ and γ run over 1–2. The comma in the subscribe denotes derivative respect to the corresponding coordinates, and the repeated indices mean a Einstein summation convention over the whole range of the index. It has been examined that the above evolution equation is equivalent to the Landau–Lifschitz–Gilbert equation [23].

The mechanical equilibrium equation and the Maxwell equation which governs the magnetic part are also incorporated:

$$\left(\frac{\partial \mathcal{H}}{\partial \varepsilon_{ij}}\right)_{,j} = 0 \quad \text{and} \quad \left(-\frac{\partial \mathcal{H}}{\partial H_j}\right)_{,j} = 0. \quad (5)$$

With the six degrees of freedom $[u_1, u_2, u_3, \phi, \vartheta_1, \vartheta_2]^{\text{T}}$, a 3D nonlinear finite element implementation is performed to solve Eqs. (3) and (5) [23]. The hcp Cobalt nanocylinder with a height h and a radius of r under mechanical strain along the longitude axis is simulated, as schematized in Fig. 1(a). The material parameters are taken as [24,25]: $C_{11} = 307$ GPa, $C_{12} = 165$ GPa, $C_{44} = 75.5$ GPa, $C_{13} = 103$ GPa, $C_{33} = 358$ GPa, $B_1 = -8.1$ MPa, $B_2 = -29$ MPa, $B_3 = 28.2$ MPa, $B_4 = 29.4$ MPa, $K_u = 6.5 \times 10^4$ J/m^3, $M_s = 1.424 \times 10^6$ A/m, $A_e = 3.3 \times 10^{-11}$ J/m, $\alpha = 0.01$. Due to the exchange length $\sqrt{2A_e/(\mu_0 M_s^2)} \approx 5.1$ nm [26], the finite element mesh size is chosen to be $\leq$2.5 nm [27].

3. Results and discussion

As a negative magnetostrictive material, hcp Cobalt requires a tensile strain to switch the magnetization initially along the strain direction. Hence, tensile strain along x_3 direction (Fig. 1(a)) is applied here. The mechanically induced switching behavior is dependent on the geometry of the nanocylinders, as shown in Fig. 1(b) and (c). When r is small, coherent switching happens where the magnetization is homogeneous all the time, as it is shown in Fig. 1(b) for the case of $r = 8$ nm. If r increases to 9 nm in Fig. 1(c), the magnetization is inhomogeneous for a period of time. In other words, incoherent switching happens. For the storage application, the coherent switching is of interest. A series of simulations have thus been performed to determine the size region, within which a coherent switching happens. As it is shown in Fig. 1(d), the maximal radius is around 8 nm when the height of the cylinder is less than 32.5 nm. When the radius is less than 7 nm, coherent switching always happens. The transition maps in Fig. 1(d) give detailed information on how to achieve different switching modes by adjusting the geometry of the nanomagnets. This is of great importance for BPM concept, in which coherent switching in nanomagnets is highly recommended. By using the transition maps, a coherent switching for BPM can be designed. For the following study, the cylinder with $r = 8$ nm, $h = 10$ nm is considered.

It is well known that for a steady-state consideration, a deterministic 90° switching can be achieved by a mechanical strain. This consensus is also confirmed by our dynamic simulations. Fig. 2(a) shows the 3D trajectories of the mechanically induced switching process. After sufficient long time, one of the four distinct magnetization states with $\vartheta_1 = 90°$, $\vartheta_2 = 45°$, 135°, 225°, and 315° can be reached. Fig. 2(a) also indicates that the final states of a stable 90° switching are highly dependent on the value of the applied strain. But this dependence seems to follow no definite laws (Fig. 2(a)), making these final stable states not suitable for reliable logic or memory states. The reason for this irregular dependence from the viewpoint of numerical simulation requires further study. But in practice, thermal fluctuation should be a possible reason. The strain for achieving 90° switching should be no less than 0.17%, as shown in Fig. 2(b). It can also be seen in Fig. 2(b) that when the strain is very small (e.g. $\varepsilon = 0.17\%$), the stable angle is larger than 90°. The possible reason is that the magneto-mechanical coupling induced magnetoelastic anisotropy in the plane of $\vartheta_1 = 90°$ is not enough to eliminate the magnetocrystalline anisotropy along the $\vartheta_1 = 0°$ direction. Thus, the overall anisotropy direction may deviate from $\vartheta_1 = 90°$. More importantly, due to the small damping ($\alpha = 0.01$), the precessional switching leads to oscillation, and ϑ_1 can run over 90°. This is totally different from the steady-state consideration, in which only a 90° switching is believed to occur. Due to the dynamic precessional switching, the maximum switching (ϑ_1^m) can reach 91°–120°. Moreover, ϑ_1^m decreases with the applied strain. The dynamic nature and overrun behavior open a whole new vista for switching magnetization with a mechanical strain.

Results show that if the strain is removed once ϑ_1 reaches 90° dynamically or steadily, there is equal possibility for the magnetization to revert back to 0° or switch by 180°. Thus no deterministic 180° switching happens. On the contrary, if the dynamic nature and overrun behavior of the magnetization are utilized, i.e. the strain is removed when ϑ_1 runs beyond 90°, a deterministic 180° switching can happen. As the optimum case, the strain is withdrawn when ϑ_1 reaches its maximum value ϑ_1^m. To demonstrate the scheme, we assume here the strain is removed instantly. The rate dependence of the loading and removal of the mechanical strain will be studied in the near future. As it is seen in Fig. 3(b), after removal of the strain, ϑ_1 is switched further to 180°. For a comparison, the case when the strain is kept is shown in Fig. 3(a). The switching mechanism is analyzed in terms of energy evolution in Fig. 3(c). During the stage with strain, i.e. from 0°–ϑ_1^m, only the magnetic–elastic coupling energy $\mathcal{H}^{\text{mag-ela}}$ decreases. This suggests the magnetic–elastic coupling is the driving force for this stage. In contrast, during the stress-free stage, the magnetocrystalline anisotropy energy $\mathcal{H}^{\text{ani}}$ is the driving force.

The dependence of the deterministic 180° switching behavior on the strain magnitude is also investigated. As shown in Fig. 4(a), all the temporal evolution of ϑ_1 under a

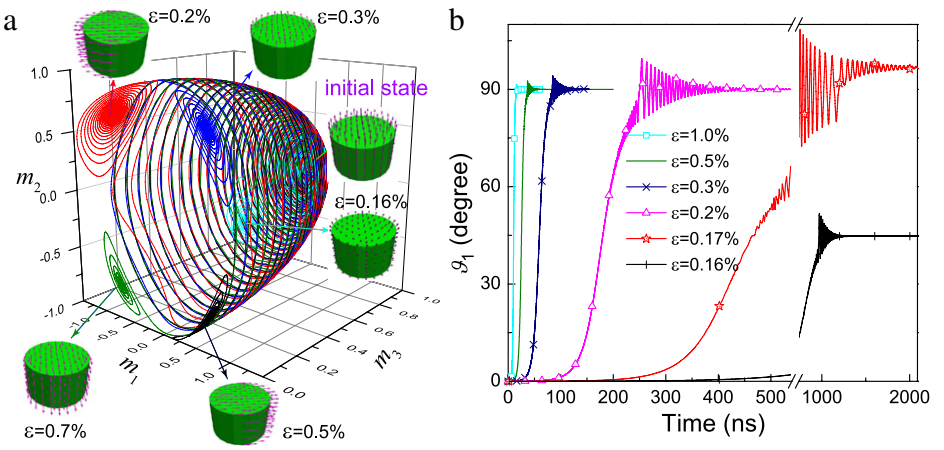

Fig. 2. (a) 3D trajectories of the magnetization vector under different strain level. The inset cylinders with arrows show the initial and final magnetization states. (b) Temporal evolution of ϑ_1 under different strain level.

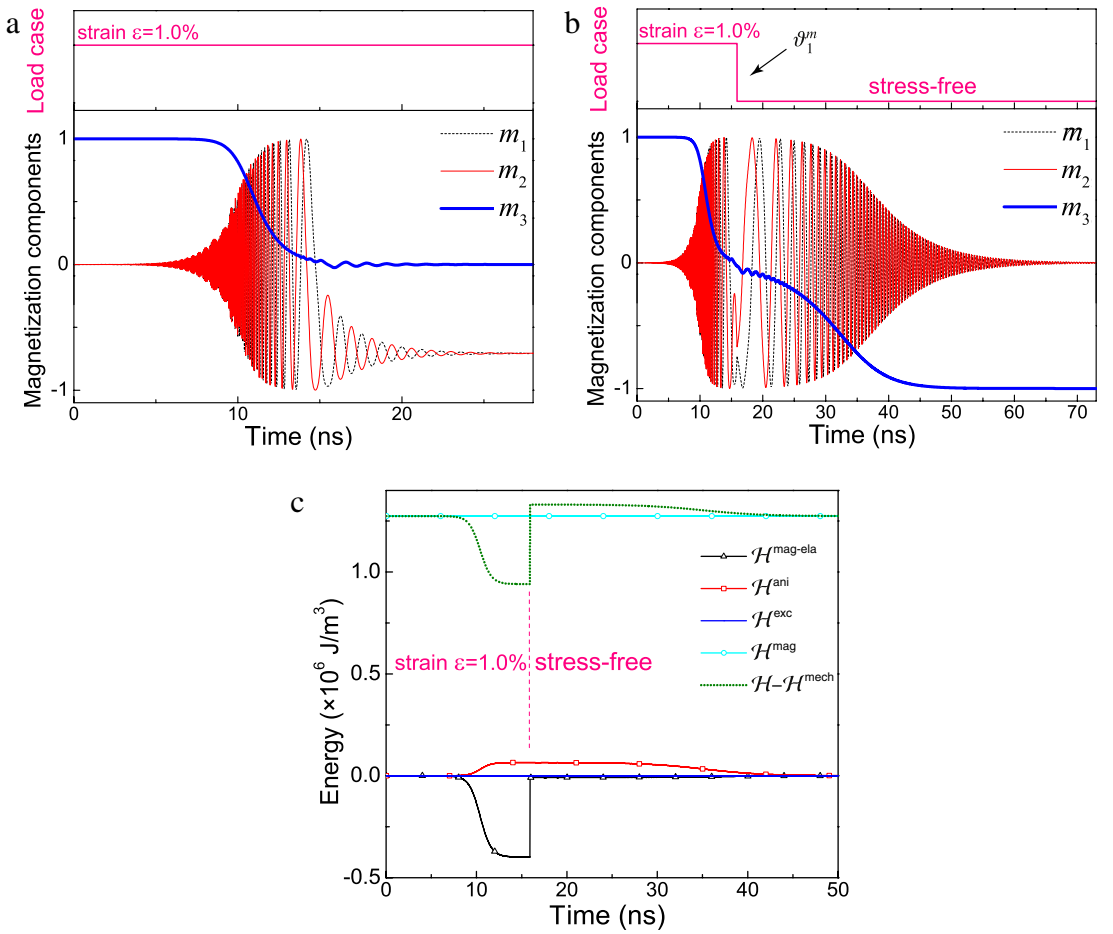

Fig. 3. Strain history and temporal evolution of magnetization components under (a) 90° and (b) 180° switching. (c) Temporal evolution of energy during a 180° switching.

strain of 0.17%–1.5% indicates an apparent 180° switching. The value of ϑ_1^m influences the switching time at the second stage without strain, i.e. from ϑ_1^m to 180°. But the total switching time from 0° to 180° is determined by the strain level: the total switching time decreases with increasing strain.

The effects of strain magnitude and magnetocrystalline anisotropy on the time for 180° switching are depicted in

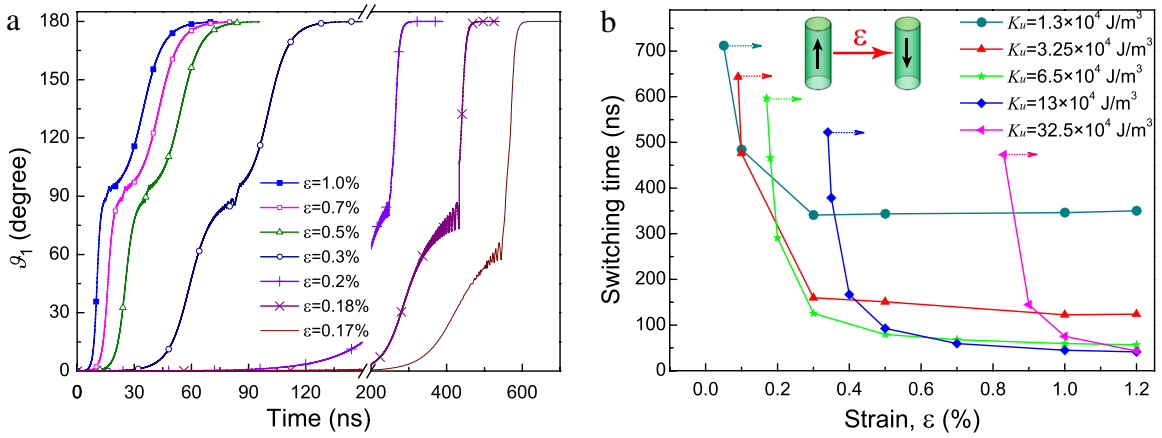

Fig. 4. (a) Temporal evolution of ϑ_1 during 180° switching under $K_u = 6.5 \times 10^4$ J/m^3. (b) The time for 180° switching as a function of strain and magnetocrystalline anisotropy. The inset dotted arrows indicate the threshold strain beyond which 180° switching happens.

Fig. 4(b). Different values of K_u changing from 1.3×10^4 to 32.5×10^4 J/m^3 are considered. For all the cases, the switching time first decreases remarkably with increasing strain and then saturates. Thus a moderate strain should be sufficient. The minimal switching time at saturation stage decreases with increasing K_u. However, it seems also to saturate after a certain level of K_u, as Fig. 4(b) shows. Large K_u favors the stability of 0° and 180° magnetization state, but increases the threshold strain for such a switching. As it is demonstrated in Fig. 4(b), the threshold strain for the case of $K_u = 1.3 \times 10^4$ J/m^3 is around 0.04%, whereas 0.83% for $K_u = 32.5 \times 10^4$ J/m^3. Hence, in order to simultaneously achieve small switching time, low threshold strain, and relatively high stability of magnetization state, Fig. 4(b) suggests that a moderate K_u between 6.5 and 13×10^4 J/m^3 seems a good choice.

It should be remarked additionally that the thermal noise is ignored in this work. But in the practical case, the thermal noise induces additional torque [6,28,29], and makes magnetization vectors fluctuate with small deviation. However, as a conservative consideration here, it is assumed that the mechanical loading is removed when ϑ_1^m is reached. If ϑ_1^m is large enough, small thermal fluctuation cannot hamper the 180° switching. The angle deflection by thermal fluctuation was reported to be around 1° [28,30]. In the work here, ϑ_1^m in all conditions is large than 91°, as shown in Fig. 2(b). Therefore, ϑ_1^m is possible to overcome the thermal fluctuation. In the near future work, quantitative study is planned for the effect of thermal noise.

It should be also mentioned that the precise withdrawal of the strain at ϑ_1^m can be a technical challenge, although it is not the intention of this work. When the mechanical loading should be removed requires a precise feedback circuit. A presumable scheme is building a magneto-tunneling junction with the magnetostrictive layer as the soft layer and monitoring its resistance. Within this scheme, the feedback circuit introduces its own errors and consumes a lot of power. Recently, Biswas et al. [12] have proposed a scheme of sequential mechanical loading by a two-phase stress, and realized the 180° switching with nearly 100% probability with strain/stress alone and without precise timing of the strain/stress cycle. This scheme should be also applicable to the study here.

4. Conclusions

In summary, our phase field simulations show that by making use of the dynamic nature and overrun behavior of the magnetization during the precessional switching, the mechanically induced deterministic 180° switching can be achieved in Cobalt nanocylinders, if mechanical strain is removed once the magnetization rotates to the achievable largest angle away from the easy axis. The switching process is firstly driven by the magneto-elastic coupling and then by the magnetocrystalline anisotropy. The threshold strain for switching increases with K_u. The investigation on switching time suggests that moderate strain and K_u are sufficient. Moreover, the cylinder size limit to ensure a coherent switching model is determined. In future work, the proposed mechanical loading scheme will be further examined in more complex situations, for instance, when strain ramp rate and temperature fluctuation are also taken into account.

Acknowledgments

The support from the China Scholarship Council, the German federal state of Hessen through its excellence programme LOEWE “RESPONSE”, and the Innovation Foundation of BUAA for Ph.D. Graduates (YWF14YJSY052) is acknowledged.

References

[1] K. Kirk, Nanomagnets for sensors and data storage, Contemp. Phys. 41 (2) (2000) 61–78. http://dx.doi.org/10.1080/001075100181187.
[2] N. Thiyagarajah, M. Asbahi, R.T. Wong, K.W. Low, N.L. Yakovlev, J.K. Yang, V. Ng, A facile approach for screening isolated nanomagnetic behavior for bit-patterned media, Nanotechnology 25 (22) (2014) 225203. http://dx.doi.org/10.1088/0957-4484/25/22/225203.
[3] M. Yi, B.-X. Xu, Z. Shen, Effects of magnetocrystalline anisotropy and magnetization saturation on the mechanically induced switching in nanomagnets, J. Appl. Phys. 117 (10) (2015) 103905. http://dx.doi.org/10.1063/1.4914485.

[4] J. Heron, M. Trassin, K. Ashraf, M. Gajek, Q. He, S. Yang, D. Nikonov, Y. Chu, S. Salahuddin, R. Ramesh, Electric-field-induced magnetization reversal in a ferromagnet-multiferroic heterostructure, Phys. Rev. Lett. 107 (21) (2011) 217202. http://dx.doi.org/10.1103/PhysRevLett.107.217202.
[5] Y.-H. Chu, L.W. Martin, M.B. Holcomb, M. Gajek, S.-J. Han, Q. He, N. Balke, C.-H. Yang, D. Lee, W. Hu, Q. Zhan, Y. Pei-Ling, A. Fraile-Rodríguez, A. Scholl, S.X. Wang, R. Ramesh, Electric-field control of local ferromagnetism using a magnetoelectric multiferroic, Nature Mater. 7 (6) (2008) 478–482. http://dx.doi.org/10.1038/nmat2184.
[6] A. Khan, D.E. Nikonov, S. Manipatruni, T. Ghani, I.A. Young, Voltage induced magnetostrictive switching of nanomagnets: strain assisted strain transfer torque random access memory, Appl. Phys. Lett. 104 (26) (2014) 262407. http://dx.doi.org/10.1063/1.4884419.
[7] M. Yi, B.-X. Xu, D. Gross, Mechanically induced deterministic 180° switching in nanomagnets, Mech. Mater. (2015) in revision.
[8] M. Fechner, P. Zahn, S. Ostanin, M. Bibes, I. Mertig, Switching magnetization by 180° with an electric field, Phys. Rev. Lett. 108 (19) (2012) 197206. http://dx.doi.org/10.1103/PhysRevLett.108.197206.
[9] S. Mangin, Y. Henry, D. Ravelosona, J. Katine, E.E. Fullerton, Reducing the critical current for spin-transfer switching of perpendicularly magnetized nanomagnets, Appl. Phys. Lett. 94 (1) (2009) 012502. http://dx.doi.org/10.1063/1.3058680.
[10] J. Katine, F. Albert, R. Buhrman, E. Myers, D. Ralph, Current-driven magnetization reversal and spin-wave excitations in Co/Cu/Co pillars, Phys. Rev. Lett. 84 (14) (2000) 3149. http://dx.doi.org/10.1103/PhysRevLett.84.3149.
[11] E. Myers, D. Ralph, J. Katine, R. Louie, R. Buhrman, Current-induced switching of domains in magnetic multilayer devices, Science 285 (5429) (1999) 867–870. http://dx.doi.org/10.1126/science.285.5429.867.
[12] A.K. Biswas, S. Bandyopadhyay, J. Atulasimha, Complete magnetization reversal in a magnetostrictive nanomagnet with voltage-generated stress: a reliable energy-efficient non-volatile magneto-elastic memory, Appl. Phys. Lett. 105 (7) (2014) 072408. http://dx.doi.org/10.1063/1.4893617.
[13] M.S. Fashami, K. Roy, J. Atulasimha, S. Bandyopadhyay, Magnetization dynamics, bennett clocking and associated energy dissipation in multiferroic logic, Nanotechnology 22 (15) (2011) 155201. http://dx.doi.org/10.1088/0957-4484/22/15/155201.
[14] S. Sahoo, S. Polisetty, C.-G. Duan, S.S. Jaswal, E.Y. Tsymbal, C. Binek, Ferroelectric control of magnetism in $BaTiO_3$/Fe heterostructures via interface strain coupling, Phys. Rev. B 76 (9) (2007) 092108. http://dx.doi.org/10.1103/PhysRevB.76.092108.
[15] J. Atulasimha, S. Bandyopadhyay, Bennett clocking of nanomagnetic logic using multiferroic single-domain nanomagnets, Appl. Phys. Lett. 97 (17) (2010) 173105. http://dx.doi.org/10.1063/1.3506690.
[16] N. Pertsev, H. Kohlstedt, Magnetic tunnel junction on a ferroelectric substrate, Appl. Phys. Lett. 95 (16) (2009) 163503. http://dx.doi.org/10.1063/1.3253706.
[17] J.-M. Hu, C. Nan, Electric-field-induced magnetic easy-axis reorientation in ferromagnetic/ferroelectric layered heterostructures, Phys. Rev. B 80 (22) (2009) 224416. http://dx.doi.org/10.1103/PhysRevB.80.224416.
[18] W. Eerenstein, N. Mathur, J. Scott, Multiferroic and magnetoelectric materials, Nature 442 (7104) (2006) 759–765. http://dx.doi.org/10.1038/nature05023.
[19] C.-W. Nan, M. Bichurin, S. Dong, D. Viehland, G. Srinivasan, Multiferroic magnetoelectric composites: historical perspective, status, and future directions, J. Appl. Phys. 103 (3) (2008) 031101. http://dx.doi.org/10.1063/1.2836410.
[20] K. Roy, S. Bandyopadhyay, J. Atulasimha, Hybrid spintronics and straintronics: a magnetic technology for ultra low energy computing and signal processing, Appl. Phys. Lett. 99 (6) (2011) 063108. http://dx.doi.org/10.1063/1.3624900.
[21] S. Geprags, A. Brandlmaier, M. Opel, R. Gross, S. Goennenwein, Electric field controlled manipulation of the magnetization in Ni/$BaTiO_3$ hybrid structures, Appl. Phys. Lett. 96 (14) (2010) 142509. http://dx.doi.org/10.1063/1.3377923.
[22] N. Pertsev, H. Kohlstedt, Resistive switching via the converse magnetoelectric effect in ferromagnetic multilayers on ferroelectric substrates, Nanotechnology 21 (47) (2010) 475202. http://dx.doi.org/10.1088/0957-4484/21/47/475202.
[23] M. Yi, B.-X. Xu, A constraint-free phase field model for ferromagnetic domain evolution, Proc. R. Soc. A 470 (2171) (2014) 20140517. http://dx.doi.org/10.1098/rspa.2014.0517.
[24] D. Sander, The correlation between mechanical stress and magnetic anisotropy in ultrathin films, Rep. Progr. Phys. 62 (5) (1999) 809. http://dx.doi.org/10.1088/0034-4885/62/5/204.
[25] J. Rothman, M. Kläui, L. Lopez-Diaz, C. Vaz, A. Bleloch, J. Bland, Z. Cui, R. Speaks, Observation of a bi-domain state and nucleation free switching in mesoscopic ring magnets, Phys. Rev. Lett. 86 (6) (2001) 1098. http://dx.doi.org/10.1103/PhysRevLett.86.1098.
[26] G.S. Abo, Y.-K. Hong, J.-H. Park, J.-J. Lee, W. Lee, B.-C. Choi, Definition of magnetic exchange length, IEEE Trans. Magn. 49 (8) (2013) 4937–4939. http://dx.doi.org/10.1109/TMAG.2013.2258028.
[27] H. Szambolics, L. Buda-Prejbeanu, J.-C. Toussaint, O. Fruchart, A constrained finite element formulation for the Landau–Lifshitz–Gilbert equations, Comput. Mater. Sci. 44 (2) (2008) 253–258. http://dx.doi.org/10.1016/j.commatsci.2008.03.019.
[28] D.E. Nikonov, G.I. Bourianoff, G. Rowlands, I.N. Krivorotov, Strategies and tolerances of spin transfer torque switching, J. Appl. Phys. 107 (11) (2010) 113910. http://dx.doi.org/10.1063/1.3429250.
[29] K. Roy, S. Bandyopadhyay, J. Atulasimha, Energy dissipation and switching delay in stress-induced switching of multiferroic nanomagnets in the presence of thermal fluctuations, J. Appl. Phys. 112 (2) (2012) 023914. http://dx.doi.org/10.1063/1.4737792.
[30] K. Roy, S. Bandyopadhyay, J. Atulasimha, Switching dynamics of a magnetostrictive single-domain nanomagnet subjected to stress, Phys. Rev. B 83 (22) (2011) 224412. http://dx.doi.org/10.1103/PhysRevB.83.224412.